The Astronomical Journal, 152:212 (8pp), 2016 December
doi:10.3847/0004-6256/152/6/212

OSSOS. IV. DISCOVERY OF A DWARF PLANET CANDIDATE IN THE 9:2 RESONANCE WITH NEPTUNE

Michele T. Bannister[1,5,10], Mike Alexandersen[2], Susan D. Benecchi[3], Ying-Tung Chen[2], Audrey Delsanti[4], Wesley C. Fraser[5], Brett J. Gladman[6], Mikael Granvik[7], Will M. Grundy[8], Aurélie Guilbert-Lepoutre[9], Stephen D. J. Gwyn[10], Wing-Huen Ip[11,12], Marian Jakubik[13], R. Lynne Jones[14], Nathan Kaib[15], J. J. Kavelaars[1,10], Pedro Lacerda[5], Samantha Lawler[10], Matthew J. Lehner[2,16,17], Hsing Wen Lin[11], Patryk Sofia Lykawka[18], Michael Marsset[4,19], Ruth Murray-Clay[20], Keith S. Noll[21], Alex Parker[22], Jean-Marc Petit[9], Rosemary E. Pike[1,2], Philippe Rousselot[9], Megan E. Schwamb[23], Cory Shankman[1], Peter Veres[24], Pierre Vernazza[4], Kathryn Volk[25], Shiang-Yu Wang[2], and Robert Weryk[26]

[1] Department of Physics and Astronomy, University of Victoria, Elliott Building, 3800 Finnerty Road, Victoria, BC V8P 5C2, Canada; michele.t.bannister@gmail.com
[2] Institute for Astronomy & Astrophysics, Academia Sinica; 11F AS/NTU, National Taiwan University, 1 Roosevelt Road, Sec. 4, Taipei 10617, Taiwan
[3] Planetary Science Institute, 1700 East Fort Lowell, Suite 106, Tucson, AZ 85719, USA
[4] Aix Marseille Université, CNRS, LAM (Laboratoire d'Astrophysique de Marseille) UMR 7326, F-13388, Marseille, France
[5] Astrophysics Research Centre, Queen's University Belfast, Belfast BT7 1NN, UK
[6] Department of Physics and Astronomy, University of British Columbia, Vancouver, BC, Canada
[7] Department of Physics, P.O. Box 64, 00014 University of Helsinki, Finland
[8] Lowell Observatory, Flagstaff, AZ, USA
[9] Institut UTINAM UMR6213, CNRS, Univ. Bourgogne Franche-Comté, OSU Theta F-25000 Besançon, France
[10] NRC-Herzberg Astronomy and Astrophysics, National Research Council of Canada, 5071 West Saanich Road, Victoria, BC V9E 2E7, Canada
[11] Institute of Astronomy, National Central University, Taiwan
[12] Space Science Institute, Macau University of Science and Technology, Macau
[13] Astronomical Institute, Slovak Academy of Science, 05960 Tatranska Lomnica, Slovakia
[14] University of Washington, Washington, USA
[15] HL Dodge Department of Physics & Astronomy, University of Oklahoma, Norman, OK 73019, USA
[16] Department of Physics and Astronomy, University of Pennsylvania, 209 S. 33rd Street, Philadelphia, PA 19104, USA
[17] Harvard-Smithsonian Center for Astrophysics, 60 Garden Street, Cambridge, MA 02138, USA
[18] Astronomy Group, School of Interdisciplinary Social and Human Sciences, Kindai University, Japan
[19] European Southern Observatory (ESO), Alonso de Córdova 3107, 1900 Casilla Vitacura, Santiago, Chile
[20] Department of Physics, University of California, Santa Barbara, CA 93106, USA
[21] NASA Goddard Space Flight Center, Code 693, Greenbelt, MD 20771, USA
[22] Southwest Research Institute, Boulder, CO, USA
[23] Gemini Observatory, Northern Operations Center, 670 North A'ohoku Place, Hilo, HI 96720, USA
[24] Jet Propulsion Laboratory, California Institute of Technology, Pasadena, CA 91109, USA
[25] Department of Planetary Sciences/Lunar & Planetary Laboratory, University of Arizona, 1629 E University Boulevard, Tucson, AZ 85721, USA
[26] Institute for Astronomy, University of Hawaii, 2680 Woodlawn Drive, Honolulu HI 96822, USA
Received 2016 July 22; revised 2016 September 28; accepted 2016 October 4; published 2016 December 5

ABSTRACT

We report the discovery and orbit of a new dwarf planet candidate, 2015 RR_{245}, by the Outer Solar System Origins Survey (OSSOS). The orbit of 2015 RR_{245} is eccentric ($e = 0.586$), with a semimajor axis near 82 au, yielding a perihelion distance of 34 au. 2015 RR_{245} has $g - r = 0.59 \pm 0.11$ and absolute magnitude $H_r = 3.6 \pm 0.1$; for an assumed albedo of $p_V = 12\%$, the object has a diameter of ~670 km. Based on astrometric measurements from OSSOS and Pan-STARRS1, we find that 2015 RR_{245} is securely trapped on ten-megayear timescales in the 9:2 mean-motion resonance with Neptune. It is the first trans-Neptunian object (TNO) identified in this resonance. On hundred-megayear timescales, particles in 2015 RR_{245}-like orbits depart and sometimes return to the resonance, indicating that 2015 RR_{245} likely forms part of the long-lived metastable population of distant TNOs that drift between resonance sticking and actively scattering via gravitational encounters with Neptune. The discovery of a 9:2 TNO stresses the role of resonances in the long-term evolution of objects in the scattering disk and reinforces the view that distant resonances are heavily populated in the current solar system. This object further motivates detailed modeling of the transient sticking population.

Key words: Kuiper belt objects: individual (2015 RR245)

1. INTRODUCTION

The Outer Solar System Origins Survey (OSSOS) was designed to provide a set of 500+ very precise trans-Neptunian object (TNO) orbits by the end of its 2013–2017 observations with the Canada–France–Hawaii Telescope (CFHT) (Bannister et al. 2016). As OSSOS covers 155 square degrees of sky on and near the solar system midplane, the Kuiper Belt's steep luminosity function (Gladman et al. 2001; Petit et al. 2011; Fraser et al. 2014) was used to predict that the brightest target expected to be found over the course of the survey would have an apparent magnitude of $m_r \sim 21.5$. At $m_r = 21.8$, 2015 RR_{245} is the brightest target discovered by OSSOS. At a current heliocentric distance of 65 au, this bright OSSOS detection is also far beyond the median distance of TNO detections in sky surveys. Its substantial distance requires 2015 RR_{245} to be sizable.

2. DISCOVERY AND SIZE

2015 RR_{245} was discovered with apparent mean magnitude $m_r = 21.76 \pm 0.01$ in three images taken with the CFHT

Table 1
Selected Observations with the CFHT MegaCam of 2015 RR_{245}

Time (UT)	Filter	Exposure Time (s)	Magnitude	IQ ($''$)	Target Elongation (°)
2015 09 09.37654	R.MP9602	300	21.77 ± 0.02	0.42	159.3
2015 09 09.42092	R.MP9602	300	21.77 ± 0.02	0.42	159.3
2015 09 09.46188	R.MP9602	300	21.73 ± 0.02	0.42	159.4
2016 02 04.22299	R.MP9602	200	22.04 ± 0.06	1.21	51.4
2016 02 04.22679	G.MP9402	200	22.63 ± 0.07	1.56	51.4
2016 06 07.61302	R.MP9602	300	21.94 ± 0.03	0.55	69.5
2016 06 08.57085	R.MP9602	300	21.88 ± 0.02	0.60	70.4

Note. The photometry is calibrated to the SDSS per the methodology in Bannister et al. (2016). The filter bandpasses are similar to those of Sloan.

MegaCam in an r-band filter over a two-hour span on 2015 September 9 (Table 1). The TNO was found within the 21 deg^2 survey region centered at R.A. 0^h30^m, decl. $+5\overset{\circ}{.}0$, the seventh of the eight OSSOS survey areas. The discovery analysis was as described in Bannister et al. (2016). 2015 RR_{245} is a characterized discovery within OSSOS: its discovery magnitude is within the range where the survey has a calibrated detection efficiency and full tracking of all discoveries to a high-precision orbit was possible. A full debiasing of the region's discoveries will be accomplished using the OSSOS survey simulator (Bannister et al. 2016) in the future. Because OSSOS reduces an entire discovery semester of data after the semester's observations are complete, the software first yielded the object in late 2016 January. OSSOS imaging is designed to provide tracking throughout the discovery semester; these data quickly yielded further astrometry in 2015 September through December.

In 2016 February, just before 2015 RR_{245} moved close to solar conjunction, a sequential pair of images in g and r (Table 1) yielded a preliminary broadband color of $g - r = 0.59 \pm 0.11$. The relatively neutral color (compare the solar $g - r = 0.44 \pm 0.02$)[27] is more common to a dynamically excited "hot" Kuiper Belt object rather than that found in the cold classical belt (Doressoundiram et al. 2005; Peixinho et al. 2015).

We reobserved 2015 RR_{245} in early 2016 June as part of planned OSSOS recovery observations for the fields observed in 2015. 2015 RR_{245} was found to have $m_r \sim 21.8$ (Table 1), consistent with the brightness found in the 2015 September discovery observations. All measurements can be retrieved from the IAU Minor Planet Center (MPC)[28]; photometry referred to here is summarized in Table 1.

Based on the heliocentric distance (see Section 3), the absolute magnitude H_r is 3.6 ± 0.1 ($H_V = 3.8 \pm 0.1$).[29] The albedos for $2 < H_V < 4$ TNOs that have been determined by thermal measurements range between $p_V = 7\%$ (2002 MS_4; $H_V = 4.0$) and 21% (Quaoar; $H_V = 2.7$) (Brucker et al. 2009). For an assumed albedo p_V at each end of this range, less or more reflective, respectively, the diameter of 2015 RR_{245} is 870–500 km. For an albedo of 9% like that of $H_V = 2.0$ TNO 2007 OR_{10} (Pal et al. 2016), which is on a comparable orbit ($a = 67$ au, $q = 33$ au) at a current distance of 88 au (Schwamb et al. 2010), 2015 RR_{245}'s diameter would be 770 km. The neutral color of 2015 RR_{245} leans it toward being part of the neutral color class, which has lower albedos of ~6% (Lacerda et al. 2014). However, because of the wide range of albedos seen for objects in this H_V range (Lellouch et al. 2013), we adopt a modal albedo of $p_V = 12\%$ ($D \sim 670$ km) in the rest of this discussion.

The plausible diameter range for 2015 RR_{245} is interesting because it spans the range of sizes where significant changes occur in TNO surface composition, particularly with the presence of deep water ice absorption (Brown 2012). At this size scale, objects with the expected ice/rock compositional mix predominant in the outer solar system are expected to adjust to an approximately spherical hydrostatic equilibrium shape (Tancredi & Favre 2008; Lineweaver & Norman 2010). The majority of the possible diameter range places 2015 RR_{245} in the size range where self-gravity produces a spherical shape. By this criterion it could be considered one of the roughly 20–30 "dwarf planet candidates" now known from previous wide-field shallow surveys covering most of the sky (Trujillo & Brown 2003; Larsen et al. 2007; Schwamb et al. 2010; Sheppard et al. 2011; Rabinowitz et al. 2012; Bannister 2013; Brown et al. 2015), most of which have $a < 50$ au.

3. ORBIT

With all available OSSOS astrometry from 2015 September to 2016 June, the distance to 2015 RR_{245} could be accurately evaluated as 64.479 ± 0.008 au. However, the barycentric orbital semimajor axis was less precisely determinable: $a = 82.1 \pm 2.5$ au (1σ covariance-based error estimate). With a swath of semimajor axis uncertainty more than 5 au wide, it was impossible to confidently determine resonance occupation: typical resonance widths are 0.5–1 au in the outer solar system. Without a very precise orbit, multiple dynamical behaviors are possible, and this object could not usefully advance the discussion of the subtleties of resonance sticking below. At this point the object was released to the MPC so that the worldwide community could participate in the second year of recovery and provide physical characterization. On 2016 July 13, the Pan-STARRS1 survey (Kaiser et al. 2010) released six oppositions of astrometry of 2015 RR_{245} to the MPC, spanning 2010 September to 2015 July. A subset of these observations was found independently by the analysis of Weryk et al. (2016); they were augmented with additional Pan-STARRS1 detections found based on the Weryk et al. (2016) orbit.

The orbital solution to the seven-opposition set of astrometric measurements (calculated per Bernstein & Khushalani

[27] http://www.sdss.org/dr12/algorithms/ugrizvegasun/
[28] http://www.minorplanetcenter.net/db_search/show_object?utf8=%E2%9C%93&object_id=2015+RR245
[29] $H_V = H_r - 0.03 + 0.45(g - r)$ (Smith et al. 2002).

Table 2
Barycentric Elements for 2015 RR_{245} in International Celestial Reference System (ICRS) at Osculating Epoch 2457274.9

a (au)	e	i (°)	Ω (°)	ω (°)	JD peri
81.86 ± 0.05	0.5859 ± 0.0003	7.553 ± 0.001	211.761 ± 0.002	260.817 ± 0.012	2485409 ± 10

Note. Barycentric distance: 64.479 ± 0.001 au with true anomaly $f = 253^\circ.5$. Here, Ω is the longitude of the ascending node, ω the argument of perihelion, and *JD peri* is the Julian day of osculating barycentric perihelion. The uncertainties are the 1σ estimates based on the covariance matrix at the best-fit orbit, derived by the method of Bernstein & Khushalani (2000).

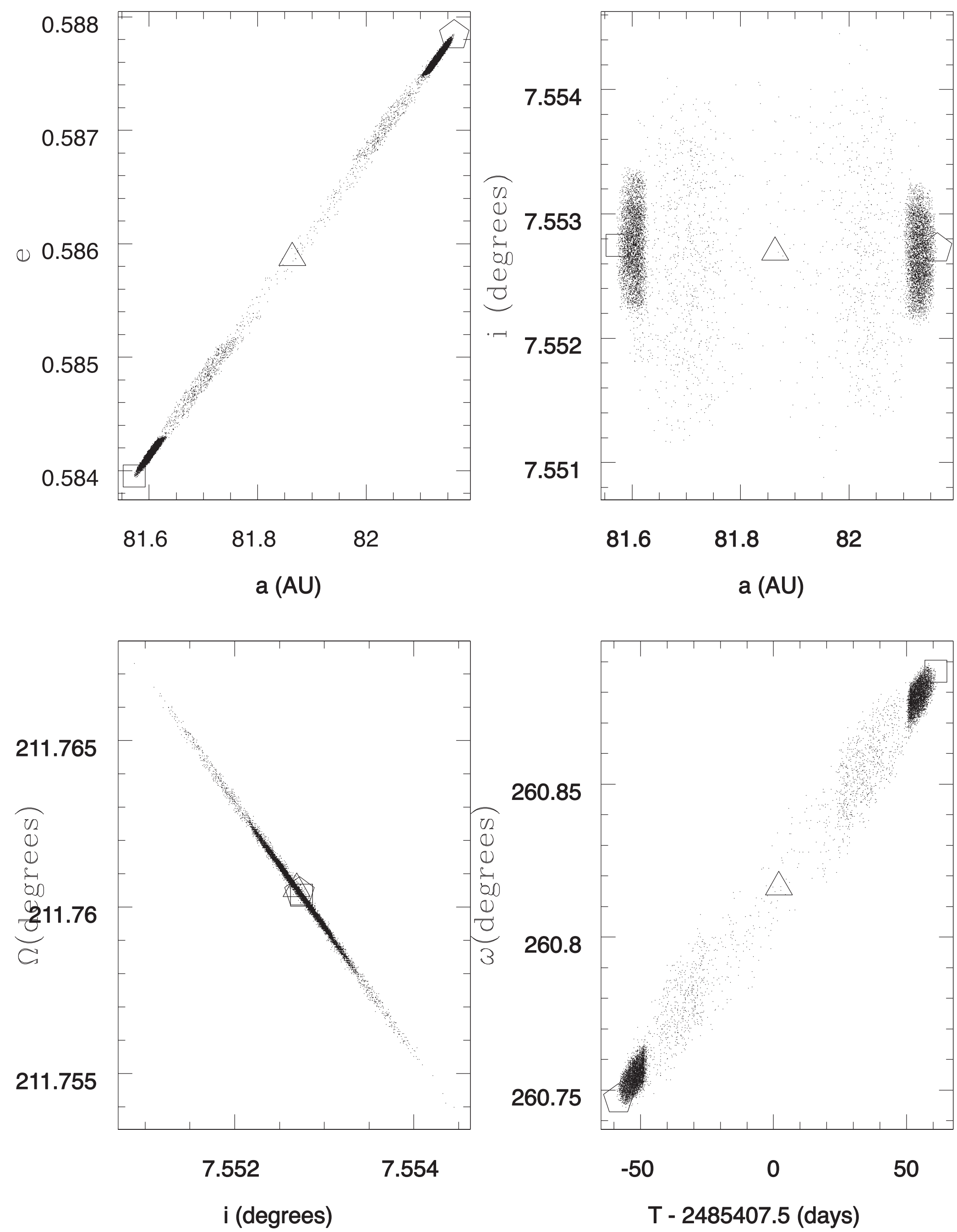

Figure 1. Uncertainties on the orbit of 2015 RR_{245} using the accounting for possible systematics fully described in Gladman et al. (2008). The best-fit orbit (Table 2) is marked by the large open triangle in each panel, while the square and pentagon give orbital elements corresponding to the minimal and maximal semimajor axes, respectively, of the Monte Carlo search. Small dots show orbits consistent with the available astrometry found during the search for the two extremal orbits; their density is not proportional to likelihood, and they are not used elsewhere in this manuscript. All elements are barycentric in the J2000 reference frame and thus judged relative to the ecliptic. Upper left: semimajor axis a vs. eccentricity e. Note the strong correlation that is equivalent to a set of orbits having nearly the same $q = 33.9$ au perihelion distance as the best-fit orbit. Upper right: ecliptic inclination i as a function of a. Lower left: longitude of ascending node Ω as a function of i. Lower right: argument of perihelion ω vs. the Julian day of osculating perihelion judged at the epoch JD = 2457274.9.

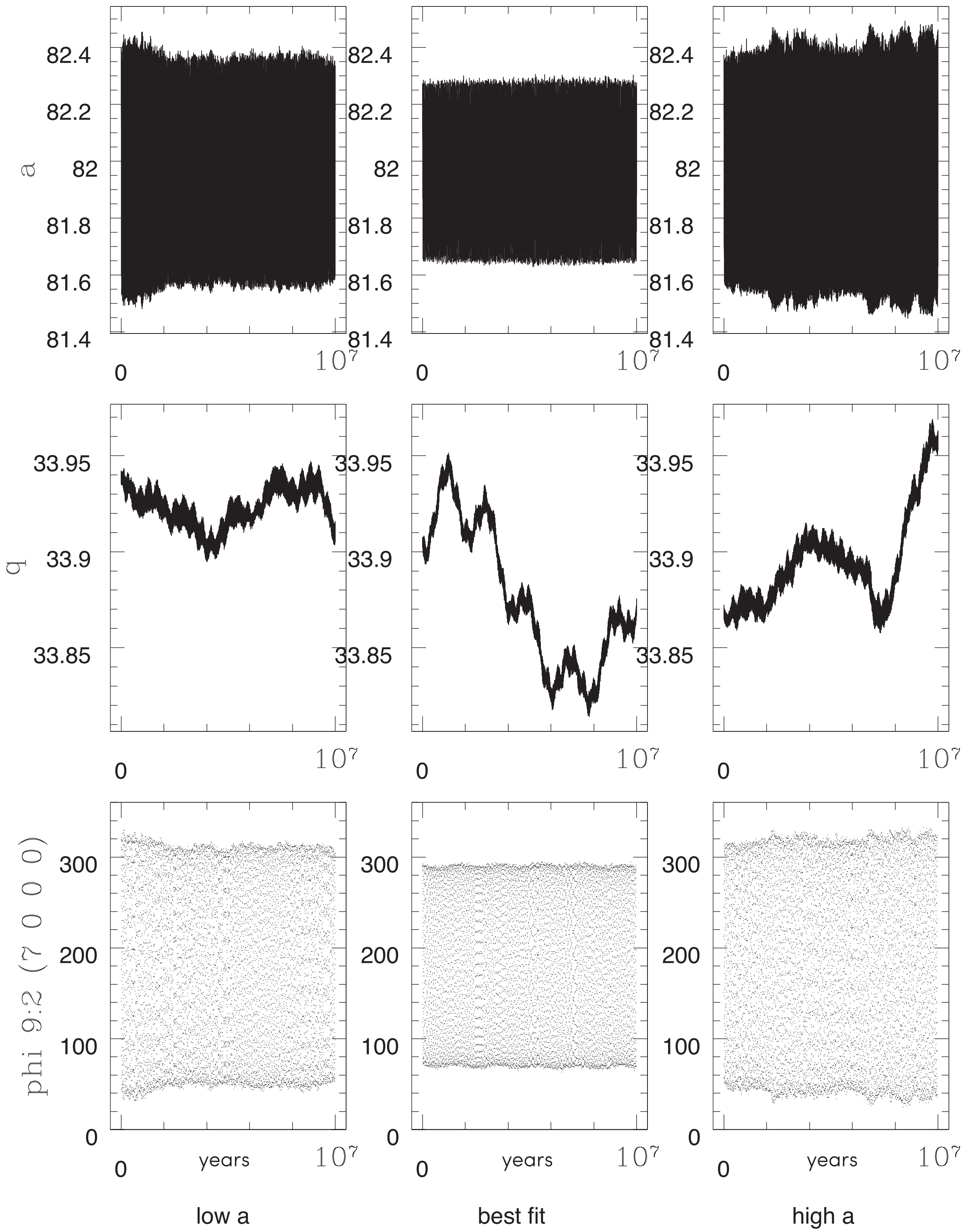

Figure 2. The orbital evolution of the three orbits marked in Figure 1. The left, middle, and right columns show the a, q, and resonant argument Φ evolution for the minimal, best-fit, and maximal semimajor axis orbits, respectively. The $\simeq$0.5 au oscillation of a is forced by the resonance and is coupled to the rapid ($\simeq$10,000 year) libration of the resonant argument. The dynamical protection provided by the resonance results in only very weak interactions, allowing only very slow evolution of the perihelion distance q. The libration amplitude in the resonance is $\simeq$110° for the best-fit orbit and is 20°–30° larger for the extremal orbits.

2000) provides a secure classification when analyzed with the dynamical orbital classification algorithm of Gladman et al. (2008): all plausible orbits yield the same dynamical behavior. The best-fit J2000 barycentric orbital elements are given in Table 2. Figure 1 shows the large span of all plausible orbital elements obtained by the Metropolis algorithm described by Gladman et al. (2008). The span of plausible orbital behaviors gives a secure dynamical classification in the 9:2 mean-motion

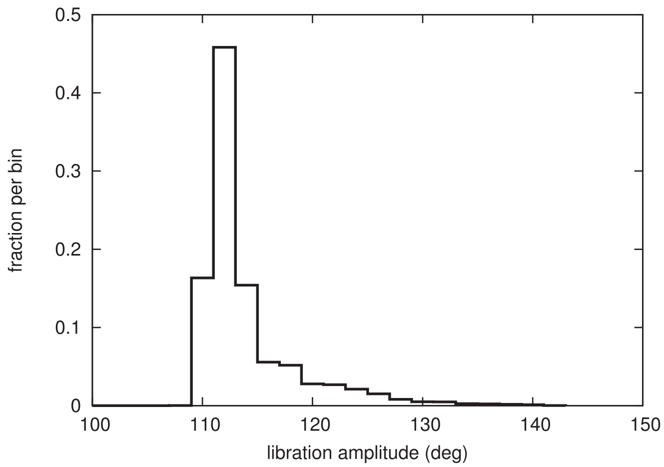

Figure 3. Histogram of the L_{92} libration amplitude distribution of the 250 clones produced by the covariance matrix analysis. See text for discussion.

resonance with Neptune (Figure 2), which is centered[30] at a barycentric semimajor axis of 81.96 au. 2015 RR_{245} is the first trans-Neptunian object securely identified in this distant resonance.

This resonance occupancy reinforces the finding that there are many TNOs in high-order, distant $a > 50$ resonances (Chiang et al. 2003; Lykawka & Mukai 2007a; Gladman et al. 2008; 2012; Alexandersen et al. 2014; Pike et al. 2015; Kaib & Sheppard 2016; Sheppard et al. 2016). Objects in large-a resonances are inefficiently discovered due to the r^{-4} dependence for reflected flux, the overall steep TNO luminosity function, and because the large eccentricities of such orbits place most of the population at large distances at any given time and thus below the flux limit of wide-field surveys. When carefully debiased for detectability, the large-a resonances together yield a total resonant population that is comparable to the main classical Kuiper Belt (Gladman et al. 2012; Pike et al. 2015; Volk et al. 2016).

The resonant protection provided by the 9:2 resonance is very similar to that provided by the 3:2 and 5:2 mean-motion resonances (Cohen & Hubbard 1965; Gladman et al. 2012). Specifically, libration of the resonant argument $\Phi_{92} = 9\lambda - 2\lambda_N - 7\varpi$ around 180° (Figure 2) means that when a resonant TNO is at perihelion, Neptune is never near the same mean orbital longitude λ_N, preventing close encounters (in this expression, λ is the mean longitude of the particle and $\varpi = \Omega + \omega$ is the longitude of perihelion). The libration amplitude L_{92} results in the perihelion longitude offset between the TNO and Neptune varying from $90° - L_{92}/2$ to $90° + L_{92}/2$. Using methods described in Volk et al. (2016), the L_{92} distribution (Figure 3) was determined with 10 Myr simulations of 250 particles ("clones") distributed probabilistically in the 3σ error ellipse card on the covariance matrix based on the orbit best fit. All these orbits remained resonant for the 10 Myr duration; at the current epoch, 2015 RR_{245} is thus firmly lodged in the resonance.

There are many resonant TNOs with precisely known orbits that are stable for the lifetime of the solar system, Pluto being an obvious example. There also exist TNOs with similar high-precision orbits whose orbital evolution shows many resonant librations for all clones initially, but then have nearly all clones leave the resonance on timescales $\ll$4 Gyr. Several Neptune 1:1 resonators (Trojans) are known to exhibit this phenomenon (Horner & Lykawka 2012; Alexandersen et al. 2014), as do three well-studied TNOs in the 5:1 (Pike et al. 2015). It is thus important to keep in mind the distinction between (1) actively "scattering" TNOs, (2) "temporarily" metastable TNOs, (3) stable resonators, and (4) permanently detached TNOs with no chance of recoupling on solar system timescales; orbital resonances are often involved when TNOs transit between those states.

To explore the longer-term evolution of 2015 RR_{245}, we extended the integration of these same 250 clones to 500 Myr. While every orbit initially spends at least 10 Myr steadily librating in the resonance, the clones begin to diffuse out on timescales of 50 Myr and begin actively scattering due to Neptune (Figure 4). Their subsequent evolution then becomes diffusive, with the scattering particles sometimes temporarily sticking to other resonances (during which the evolution shows a stable semimajor axis at some other value). Particles commonly return to stick to the 9:2 resonance itself, and then they remain stuck for typical timescales of tens of megayears. We find a median dynamical lifetime before first departure

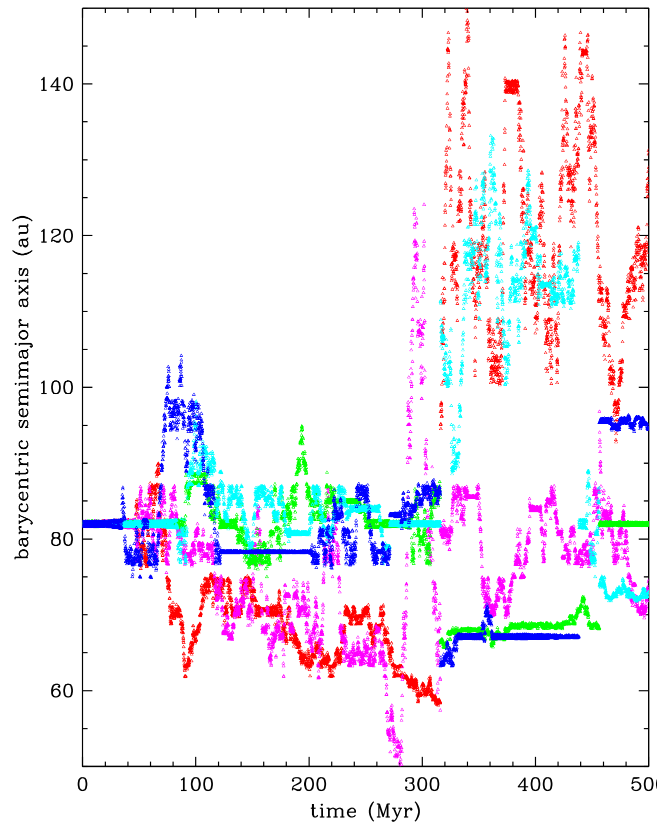

Figure 4. Semimajor axis evolution for five sample orbits (each a different color) drawn from a covariance-based set of 250 orbits consistent with the astrometry of 2015 RR_{245}. For the first 40 Myr, all 250 clones oscillate by the $\simeq$1 au full width of the resonance. They then begin leaving the resonance into the actively scattering population, where their semimajor axes are changing by several au/Myr in a diffusive manner driven by Neptune scattering. The median time before first departure from the resonance is $\simeq$100 Myr; here five orbits with less-typical early departures are shown, sometimes displaying the frequently seen behavior among the clone ensemble of subsequent sticking to other resonances or return to the 9:2.

[30] Note that this evaluation should be made in barycentric orbital element space. Neptune's barycentric semimajor axis $a_N = 30.07$ au is perturbed by up to 0.02 au on 500 Myr timescales. For instance, while the barycentric mean center of the resonance is shifting on the 10 Myr interval in Figure 2 (upper row), it is not apparent due to being $\sim$1/200th the barycentric oscillation of the particles.

from the resonance of order 100 Myr, with roughly 15% of the clones in the resonance 500 Myr in the future (note that some may have left and returned; Figure 4). Only a tiny fraction of the clones will be in the 9:2 after 4 Gyr. It is thus very likely that 2015 RR_{245} has not continuously spent the last 4 Gyr in the resonance, but instead was trapped from the actively scattering population within the last ∼100 Myr.

4. DISCUSSION

Two main possibilities appear likely for how 2015 RR_{245} came to be in its current orbit: first, that it was scattered off Neptune and is presently "sticking" to a resonance, with the scattering event either recent or early in solar system history; and second, 2015 RR_{245} could have been captured into the resonance during Neptune's migration. We consider each in turn.

Metastable resonant TNOs that are emplaced by "transient sticking" are an established phenomenon. The transient sticking slows orbital evolution, providing a mechanism necessary to maintain the current scattering disk, which would otherwise decay on timescales much shorter than the age of the solar system (Duncan & Levison 1997). Several studies of transient sticking report temporary captures in the 9:2 resonance (Fernández et al. 2004; Lykawka & Mukai 2007b; Almeida et al. 2009). These studies found most periods spent in the resonance are short (∼10 Myr) and with large libration amplitudes, $L_{92} > 130°$. However, occasionally their modeled particles attained smaller libration amplitudes, which lengthened their occupation in the resonance. The low-libration "sticker" objects provide an enhanced contribution to the steady-state transient population. Indeed, the simulations reported in Lykawka & Mukai (2007b) include stickers in the 9:2 resonance with L_{92} as small as the $\simeq 115°$ observed for 2015 RR_{245}. Of the particles in Lykawka & Mukai (2007b) surviving to the present time, roughly half had experienced a trapping in the 9:2 at some time, and one case kept $L_{92} < 120°$ for 700 Myr (P. Lykawka, 2016 private communication). 2015 RR_{245} plausibly fits into this "metastable TNO" paradigm.

Given the ∼100 Myr median resonant lifetime of our orbital clones, we suggest that 2015 RR_{245} is likely to be transiently alternating between Neptune mean-motion resonances and the actively scattering component of the trans-Neptunian region. This conclusion is bolstered by 2015 RR_{245}'s perihelion distance of $q = 34$ au; roughly[31] $q < 37$ au results in the continuing orbital interactions with Neptune that are shared by almost all active scatterers. In fact, nonresonant TNOs with q only 4 au from Neptune's orbital semimajor axis of 30 au typically experience sufficiently numerous strong encounters with Neptune (when the longitude of Neptune matches that of the TNO while the TNO is at perihelion) for their orbits to rapidly evolve (Morbidelli et al. 2004). Such rapidly evolving orbits, when observed at the current epoch, are classified in the scattering population (Gladman et al. 2008). Residence in the 9:2 or other resonances can temporarily shield TNOs from scattering, but eventually their orbital evolution will lead such TNOs to leave the resonance and resume active scattering. Note that there can be resonant objects (e.g., Pluto) that do not participate at all in this process on 4 Gyr timescales.

Though we consider transient sticking the most plausible origin for 2015 RR_{245}, other emplacement scenarios are possible. For example, Nice model-type histories (Levison et al. 2008) could in principle emplace objects in the 9:2 resonance directly during an early solar system upheaval event. If fortunate enough to remain stable for the subsequent ∼4 Gyr solar system age, these objects might still be present today. A numerical simulation of TNO sculpting under a Nice model-like solar system history (Pike et al. 2016) does produce a population of 9:2 resonant TNOs. However, the objects reported in Pike et al. (2016), drawn from the simulations of Brasser & Morbidelli (2013), may also be transient captures. Further work is needed to determine whether these objects were caught early and retained, or whether they are in fact transiently sticking TNOs captured later in the 4 Gyr numerical evolution.

Alternately, resonance capture during smooth migration of Neptune, even over a relatively large 10 au distance, would require an initial disk extending beyond 55 au to provide a source of TNOs for capture into resonance. While there are low-inclination TNOs beyond the 2:1 resonance that suggest that the cold classical TNO population did extend to at least 50 au (Bannister et al. 2016), 55 au would be at the larger end of the observed debris disk population (Hillenbrand et al. 2008). Because they appeal for capture into resonance occurring early in the solar system's history, both the Nice-type and the smooth migration scenarios would require that future observations of 2015 RR_{245} push its orbit to a subset of phase space more stable than that currently explored by our orbital clones; this seems unlikely given the extent of our numerical exploration.

We next consider whether our detection of a large TNO in the resonant phase of the metastable population is consistent with the population ratios between the two phases (scattering/resonant). Our initial numerical experiments suggest that—summed over all resonances—the transiently stuck population may be comparable to the population of active scatterers. This is similar to the behavior seen for the known 5:1 resonant TNOs, which typically spend half their lifetimes in various resonances and half in a scattering state (Pike et al. 2015). If so, a single transiently stuck dwarf planet candidate detection by OSSOS is consistent with our lack of detection of similarly sized active scatterers. Only a few of the well-populated distant resonances are known to contain $H < 4$ TNOs (Sheppard et al. 2011). Additionally, the classification methods of Elliot et al. (2005) and Gladman et al. (2008) both agree that with its current astrometric measurements, 2007 OR_{10} is securely in the 10:3 resonance. Because dynamical timescales are longer at large semimajor axes, transiently stuck TNOs spend more time in more distant (low-order) resonances, making the 9:2 a reasonable resonance in which to find 2015 RR_{245}.

When viewed in absolute magnitude H space, detection of an $H_r = 3.6$ TNO by OSSOS is naively a ∼4% probability using the TNO sky density estimates of Fraser et al. (2014, Figure 9). However, the H_r frequency distribution reported in Fraser et al. (2014) utilizes an empirical formulation that adjusts for the increased albedos of many large TNOs (Brown 2008, p. 335; Fraser et al. 2008, 2014). Use of that relation[32] to compute an "effective" H_r for 2015 RR_{245} results in a value of $H_{r,\mathrm{eff}} = 4.35$. At this $H_{r,\mathrm{eff}}$, our detection of one TNO in 155

[31] Orbital integration is required; see discussions in Lykawka & Mukai (2007a) and Gladman et al. (2008).

[32] The H_r mag of 2015 RR_{245} is used to estimate a size given an estimated intrinsic albedo of $p_V = 12\%$, and then an "effective" H_r mag is computed for that size using an effective albedo of 6%.

square degrees of survey coverage is in good agreement with the measured $H_{r,\mathrm{eff}}$ frequency distribution.

Concentrating on such "large" TNOs, 2015 RR_{245} spends approximately two-thirds of its orbit brighter than the shallowest magnitude limit $m_r \sim 24.5$ of any OSSOS block; even at aphelion its sky motion of $\sim 1''$/hr would be easily detectable by our survey. With such a substantial visibility fraction, a trivial estimate of the number of comparable TNOs within about 10° of the ecliptic is $(360 \times 20/155) \simeq 50$ $H_r < 3.6$ TNOs over the sky, with only a small upward correction (of <50%) for the fraction of the visibility. Demanding that these TNOs be also in the 9:2 should be viewed as dangerous "post facto" reasoning (in that the argument would apply to any subpopulation in which the single TNO was found). Instead, the perspective should be that there are 50–100 $H_r < 3.6$ TNOs in the volume inside 100 au, which seems completely plausible. Its dynamics suggest 2015 RR_{245} is one of the objects that survived the population decay in the initially scattered disk after experiencing scattering and temporary capture in multiple resonances. If of order 100 $H \lesssim 4$ TNOs exist and the "retention efficiency" over the entire outer solar system is ~1% (Duncan & Levison 1997; Nesvorny & Vokrouhlický 2016), then there would have been ~10,000 such objects present in the outer solar system at the time that the giant planets began to clear the region. This is in line with primordial estimates (Stern 1991; Stern & Colwell 1997) of ~1000 Plutos when one takes into account that Pluto-scale TNOs are only a fraction of the $H < 4$ inventory.

Viewed another way, there may still be an issue that is due to the puzzling fact that 2015 RR_{245} is roughly 3 mag brighter than the OSSOS detection limits. That is, OSSOS detects many TNOs with $m_r < 24.9$, and none are in the 9:2 resonance. We find that the $H_v = 4.7$ TNO 2003 UA_{414}, recently refound by Pan-STARRS,[33] is securely in the 9:2 and stably resonant on a 100 Myr timescale, with 100 clones evolved as in Section 3 all remaining resonant. No other published surveys suggest any smaller TNOs being detected in the 9:2. If one anchors a normal exponential magnitude distribution to 2015 RR_{245}, even restricting to its discovery distance of 65 au, there should be ~100 TNOs up to three magnitudes fainter, yet only one has been found. The problem is worsened when considering that near the $q = 34$ au perihelion distance, TNOs as faint as $H_r \simeq 9$ are visible to OSSOS, and detection of those TNOs is far more likely than finding 2015 RR_{245}. A plausible resolution of this apparent paradox is most likely that 2015 RR_{245} has an albedo that is higher than that of smaller TNOs (Stansberry et al. 2008), as suggested above, and thus this TNO does not anchor a steep exponential distribution. Considering known large TNOs on potentially "metastable" orbits, for an albedo like that of the substantially larger Eris (at a current heliocentric distance of 96 au) of $p \simeq 0.96$ (Sicardy et al. 2011), the effective H_r becomes nearly 6, and the nondetection of smaller TNOs even at perihelion is not statistically alarming. We point out, however, that the visual albedo of the 1500 km diameter 2007 OR_{10} is only 9% (Pal et al. 2016), raising doubt on whether all large TNOs have high albedos (Brown 2008, p. 335). Future thermal measurements and spectral studies of 2015 RR_{245}, which will steadily brighten as it approaches its 2090 perihelion, will inform the open question of its albedo and surface composition.

[33] Four new oppositions of observation in MPS 719376, http://www.minorplanetcenter.net/iau/ECS/MPCArchive/2016/MPS_20160719.pdf, changed the semimajor axis of 2003 UA_{414}'s orbit by nearly a factor of two.

This research was supported by funding from the National Research Council of Canada and the National Science and Engineering Research Council of Canada. The authors recognize and acknowledge the sacred nature of Maunakea and appreciate the opportunity to observe from the mountain. This project could not have been a success without the dedicated staff of the Canada–France–Hawaii Telescope (CFHT) telescope. This work is based on observations obtained with MegaPrime/MegaCam, a joint project of CFHT and CEA/DAPNIA. CFHT is operated by the National Research Council of Canada, the Institute National des Sciences de l'universe of the Centre National de la Recherche Scientifique of France, and the University of Hawaii, with OSSOS receiving additional access due to contributions from the Institute of Astronomy and Astrophysics, Academia Sinica, Taiwan. This work is based in part on data produced and hosted at the Canadian Astronomy Data Centre, with data processing and analysis performed using computing and storage capacity provided by the Canadian Advanced Network For Astronomy Research (CANFAR). MES was supported by the Gemini Observatory, which is operated by the Association of Universities for Research in Astronomy, Inc., on behalf of the international Gemini partnership of Argentina, Brazil, Canada, Chile, and the United States of America. MJ acknowledges support from the Slovak Grant Agency for Science (grant no. 2/0031/14).

Facilities: CFHT (MegaPrime), Pan-STARRS1.

Software: Python, astropy, matplotlib, scipy, numpy, supermongo, SWIFT.

REFERENCES

Alexandersen, M., Gladman, B., Kavelaars, J. J., et al. 2016, AJ, 152, 111
Almeida, A. J. C., Peixinho, N., & Correia, A. C. M. 2009, A&A, 508, 1021
Bannister, M. T. 2013, PhD thesis, RSAA, the Australian National Univ.
Bannister, M. T., Kavelaars, J. J., Petit, J.-M., et al. 2016, AJ, 152, 70
Bernstein, G., & Khushalani, B. 2000, AJ, 120, 3323
Brasser, R., & Morbidelli, A. 2013, Icar, 225, 40
Brown, M. E. 2008, in The Solar System Beyond Neptune, ed. M. A. Barucci et al. (Tucson, AZ: Univ. Arizona Press)
Brown, M. E. 2012, AREPS, 40, 467
Brown, M. E., Bannister, M. T., Schmidt, B. P., et al. 2015, AJ, 149, 69
Brucker, M. J., Grundy, W. M., Stansberry, J. A., et al. 2009, Icar, 201, 284
Chiang, E. I., Jordan, A. B., Millis, R. L., et al. 2003, AJ, 126, 430
Cohen, C. J., & Hubbard, E. C. 1965, AJ, 70, 10
Doressoundiram, A., Peixinho, N., Doucet, C., et al. 2005, Icar, 174, 90
Duncan, M. J., & Levison, H. F. 1997, Sci, 276, 1670
Elliot, J. L., Kern, S. D., Clancy, K. B., et al. 2005, AJ, 129, 1117
Fernández, J. A., Gallardo, T., & Brunini, A. 2004, Icar, 172, 372
Fraser, W. C., Brown, M. E., Morbidelli, A., Parker, A., & Batygin, K. 2014, ApJ, 782, 100
Fraser, W. C., Kavelaars, J. J., Holman, M. J., et al. 2008, Icar, 195, 827
Gladman, B., Kavelaars, J. J., Petit, J.-M., et al. 2001, AJ, 122, 1051
Gladman, B., Lawler, S. M., Petit, J.-M., et al. 2012, AJ, 144, 23
Gladman, B., Marsden, B. G., & Vanlaerhoven, C. 2008, The Solar System Beyond Neptune, ed. M. A. Barucci et al. (Tucson, AZ: Univ. Arizona Press), 43
Hillenbrand, L. A., Carpenter, J. M., Kim, J. S., et al. 2008, ApJ, 677, 630
Horner, J., & Lykawka, P. S. 2012, MNRAS, 426, 159
Kaib, N. A., & Sheppard, S. S. 2016, arXiv:1607.01777v1
Kaiser, N., Burgett, W., Chambers, K., et al. 2010, Proc. SPIE, 7733, 77330E
Lacerda, P., Fornasier, S., Lellouch, E., et al. 2014, arXiv:1406.1420v1
Larsen, J. A., Roe, E. S., Albert, C. E., et al. 2007, AJ, 133, 1247
Lellouch, E., Santos-Sanz, P., Lacerda, P., et al. 2013, A&A, 557, A60
Levison, H. F., Morbidelli, A., Vanlaerhoven, C., Gomes, R., & Tsiganis, K. 2008, Icar, 196, 258
Lineweaver, C. H., & Norman, M. 2010, arXiv:1004.1091

Lykawka, P. S., & Mukai, T. 2007a, Icar, 186, 331
Lykawka, P. S., & Mukai, T. 2007b, Icar, 192, 238
Morbidelli, A., Emel'yanenko, V. V., & Levison, H. F. 2004, MNRAS, 355, 935
Nesvorný, D., & Vokrouhlický, D. 2016, ApJ, 825, 94
Pal, A., Kiss, C., Müller, T. G., et al. 2016, arXiv:1603.03090
Peixinho, N., Delsanti, A., & Doressoundiram, A. 2015, A&A, 577, A35
Petit, J.-M., Kavelaars, J. J., Gladman, B. J., et al. 2011, AJ, 142, 131
Pike, R. E., Kavelaars, J. J., Petit, J.-M., et al. 2015, AJ, 149, 202
Pike, R. E., Lawler, S., Brasser, R., et al. 2016, in American Astronomical Society, DPS meeting #48 (Washington, D.C.: AAS), 200.07
Rabinowitz, D., Schwamb, M. E., Hadjiyska, E., & Tourtellotte, S. 2012, AJ, 144, 140
Schwamb, M. E., Brown, M. E., Rabinowitz, D. L., & Ragozzine, D. 2010, ApJ, 720, 1691
Sheppard, S. S., Trujillo, C., & Tholen, D. J. 2016, arXiv:1606.02294v1
Sheppard, S. S., Udalski, A., Trujillo, C., et al. 2011, AJ, 142, 98
Sicardy, B., Ortiz, J. L., Assafin, M., et al. 2011, Natur, 478, 493
Smith, J. A., Tucker, D. L., Kent, S., et al. 2002, AJ, 123, 2121
Stansberry, J., Grundy, W., Brown, M. E., et al. 2008, in The Solar System Beyond Neptune, ed. M. A. Barucci et al. (Tucson, AZ: Univ. Arizona Press), 161
Stern, S. A. 1991, Icar, 90, 271
Stern, S. A., & Colwell, J. E. 1997, AJ, 114, 841
Tancredi, G., & Favre, S. 2008, Icar, 195, 851
Trujillo, C. A., & Brown, M. E. 2003, EM&P, 92, 99
Volk, K., Murray-Clay, R., Gladman, B., et al. 2016, AJ, 152, 23
Weryk, R. J., Lilly, E., Chastel, S., et al. 2016, Icar, submitted (arXiv:1607.04895)